HHS Public Access

Author manuscript

Cell. Author manuscript; available in PMC 2017 January 14.

Published in final edited form as:

Cell. 2016 January 14; 164(0): 128–140. doi:10.1016/j.cell.2015.11.048.

Integrins form an expanding diffusional barrier that coordinates phagocytosis

Spencer A. Freeman[1], **Jesse Goyette**[2], **Wendy Furuya**[1], **Elliot C. Woods**[3], **Carolyn R. Bertozzi**[3], **Wolfgang Bergmeier**[4], **Boris Hinz**[5], **P. Anton van der Merwe**[2], **Raibatak Das**[6], and **Sergio Grinstein**[1,7,8]

[1]Program in Cell Biology, Hospital for Sick Children, Toronto, M5G 1X8, Canada

[2]Sir William Dunn School of Pathology, University of Oxford, Oxford OX1 3RE, UK

[3]Departments of Chemistry Stanford University Department of Chemistry, 380 Roth Way, Stanford, CA 94305-5080, USA

[4]Department of Biochemistry and Biophysics, University of North Carolina, 120 Mason Farm Road, Chapel Hill, NC 27599-7260, USA

[5]Matrix Dynamics Group, Faculty of Dentistry, University of Toronto, Toronto, M5S 3E2, Canada

[6]Department of Integrative Biology, University of Colorado, Denver, CO 80217-3364, USA

[7]Keenan Research Centre, St. Michael's Hospital, Toronto, M5S 1T8, Canada

Summary

Phagocytosis is initiated by lateral clustering of receptors, which in turn activates Src-family kinases (SFKs). Activation of SFKs requires depletion of tyrosine phosphatases from the area of particle engagement. We investigated how the major phosphatase CD45 is excluded from contact sites, using single-molecule tracking. The mobility of CD45 increased markedly upon engagement of Fcγ receptors. While individual CD45 molecules moved randomly, they were displaced from the advancing phagocytic cup by an expanding diffusional barrier. By micropatterning IgG, the ligand of Fcγ receptors, we found that the barrier extended well beyond the perimeter of the receptor-ligand engagement zone. Second messengers generated by Fcγ receptors activated integrins, which formed an actin-tethered diffusion barrier that excluded CD45. The expanding integrin wave facilitates the “zippering” of Fcγ receptors onto the target and integrates the information from sparse receptor-ligand complexes, coordinating the progression and ultimate closure of the phagocytic cup.

Phagocytosis is initiated by the lateral clustering of receptors upon association with ligands on the surface of a cognate target. Fcγ receptors, which recognize the Fc portion of IgG, are prototypical of the phagocytic response. The multiplicity of IgG molecules on the target

[8]Correspondence: Sergio Grinstein (sergio.grinstein@sickkids.ca).

surface promotes the close apposition of receptor immunotyrosine activation motifs, and the associated stimulation of Src-family kinases (SFKs) (Flannagan et al., 2012).

Phagocytes are richly endowed with membrane-associated tyrosine phosphatases, notably CD45 and CD148 (Zhu et al., 2008b). The activation of SFKs and effective tyrosine phosphorylation of receptors requires the physical removal of such phosphatases from sites of particle engagement. Accordingly, Goodridge et al. (2011) documented a striking exclusion of CD45/CD148 from phagocytic cups. A similar exclusion has been observed at the immune synapses formed by lymphoid cells (Davis and van der Merwe, 2006). Upon binding ligand, B and T cell receptors initially form microclusters that subsequently coalesce to form a central supermolecular activation centre (cSMAC) (Batista et al., 2001; Grakoui et al., 1999; Monks et al., 1998); in the process, phosphatases are displaced to the periphery of the contact site(s). Exclusion of the phosphatases has been attributed to a “squeezing” type of action, brought about by the close apposition of the membranes of the lymphoid and antigen-presenting cells that engage in synapse formation (Cordoba et al., 2013; James and Vale, 2012; van der Merwe and Dushek, 2011). The phosphatases are squeezed out of the tight confines of the contact zones by virtue of their extraordinarily large, glycosylated ectodomains that are rigid and considerably longer than the space between the adjoining membranes (Hermiston et al., 2009).

A similar size exclusion mechanism could underlie the removal of CD45 and CD148 from the phagocytic cup, since the exofacial domain of Fcγ receptors is notably shorter (≈6 nm) than that of the phosphatases (that ranges from ≈30–60 nm). However, while at immune synapses B and T cell receptors move laterally along with their cognate targets on antigen-presenting cells, facilitating large-scale clustering, phagocytic receptors are often immobilized by their ligands. The rigid nature of bacterial and fungal cell walls precludes the lateral motion of receptor-ligand complexes and hence impedes the formation of supermolecular structures akin to the cSMAC. It is therefore unclear whether the phosphatase size exclusion model deduced for the immune synapse is applicable to the phagocytic cup. In fact, it is not known whether the exclusion of CD45 and CD148 is in fact required for successful completion of phagocytosis.

We investigated the role and mechanism of exclusion of the phosphatases during Fcγ receptor-mediated phagocytosis by tracking single CD45 molecules during engagement of IgG-opsonized targets by macrophages. Our results revealed an unexpected role of integrins as progressive diffusional barriers that serve to integrate the signals emanating from immobile Fcγ receptor microclusters.

Results

Activation of Fcγ receptors increases the mobility of CD45

As described for dectin-mediated phagocytosis (Goodridge et al., 2011), we found that engagement of Fcγ receptors caused the depletion of CD45 from the phagocytic cup (Fig. 1A). The region of depletion of the phosphatase demarcated the zone where phosphotyrosine accumulated, consistent with a causal relationship.

The mechanism underlying the lateral displacement of the phosphatases from the phagocytic cup is not known. To understand the mechanism of depletion, we generated Fab fragments to track single CD45 molecules on the membrane of live macrophages. At the density used (100 ng/mL) the Fab fragments labeled resolvable single CD45 molecules: the modal fluorescence intensity of Cy3-conjugated anti-CD45 Fab fragments on the cell surface matched that of mono-dispersed Fabs attached to glass (Fig. S1).

Yamauchi et al (2012) proposed that myosin II facilitates the redistribution of CD45 during phagocytosis. This mechanism would predict directed motion of CD45 away from sites of receptor engagement. We tested this prediction by single-molecule tracking (SMT) of CD45 during phagocytosis. This required image acquisition over extended periods of time, tracking particles on a defined focal plane. To avoid photobleaching, we used biotinylated anti-CD45 Fab fragments tagged with quantum (Q)dots (Fig. 1B). Constancy of the focal plane was ensured by implementing a two-dimensional model of frustrated phagocytosis, where suspended labeled cells were allowed to sediment onto an IgG-coated coverslip. To measure the behavior of CD45 under “resting” conditions –i.e. in cells not performing phagocytosis– macrophages were instead sedimented onto BSA-coated coverslips. At the indicated times after contact with the coated surface the behavior of individual CD45 molecules was monitored, followed by feature detection and reconstruction of trajectories (Jaqaman et al., 2011). We next applied a moment scaling spectrum (MSS) analysis and assessed whether single trajectories were directed or isotropic. Contrary to the predictions made by the model of Yamauchi et al. (2012), fewer than 3% of the CD45 molecules moved linearly either at rest or during phagocytosis (Fig. 1B–C). Instead, CD45 followed isotropic trajectories generated by either confined diffusion or free diffusion.

Initiation of frustrated phagocytosis on the IgG-coated planar surface coincided with the emergence of a zone of CD45 depletion analogous to that observed during phagocytosis of 3-dimensional targets. Moreover, we found that engaging Fcγ receptors increased the fraction of CD45 undergoing free diffusion from 47%±14% to 70%±11% (means ± SD), at the expense of confined molecules, which decreased proportionately (Fig. 1C). Not only did the fraction of confined molecules decrease, but those that remained confined were able to roam within a larger area; the mean diameter of the remaining confinement zones increased from 171 nm to 269 nm (Fig. 1D). As a result of these combined effects, the overall diffusion coefficient increased from 0.026±0.011 $\mu m^2/s$ to 0.053±0.019 $\mu m^2/s$ (Fig. 1E). These changes were recapitulated in BSA-adherent cells by a brief treatment with latrunculin (Fig. 1C–D), suggesting that engagement of Fcγ receptors induces the breakdown of actin-based cytoskeletal barriers to CD45 diffusion. Virtually identical results were obtained in cultured murine macrophages (Fig. S1E–G) and, importantly, also in murine bone marrow-derived macrophages (BMDMs) using anti-CD45 Fab fragments directly labeled with Cy3B (Fig. S1B–D). This implies that the mobility of CD45 was not adversely affected by the Qdots, and suggest that the mobilization and depletion of CD45 from the cup occurs by a similar mechanism in multiple phagocytic cell types.

CD45 is progressively displaced by a diffusion barrier

While the MSS analysis identified the majority of the CD45 molecules as diffusing freely, perusal of individual trajectories over extended periods revealed a unique feature: the phosphatase molecules appeared to collide and bounce off the edge of the zone of depletion (Video 1; Fig. 1F). This suggested the existence of a diffusional barrier that expands as the phagocytic cup grows, progressively displacing (excluding) CD45 from the area of receptor engagement. These observations were recapitulated when CD45 was labeled with Cy3B-conjugated Fab fragments, which are considerably smaller than CD45 itself (Fig. S1B). Therefore, is it likely that the observed exclusion is an intrinsic property of the phosphatase.

We asked if single molecule trajectories could reveal the existence of a diffusional barrier. To create well-defined barriers, we printed IgG onto glass coverslips, generating ≈ 2 μm-sized circles separated by 6 μm, as done previously (Torres et al., 2008), and tracked single CD45 molecules in their vicinity. We compared observed trajectories with simulated trajectories undergoing Brownian diffusion in the presence of a diffusional barrier (Fig. 2A). The simulated barrier enclosed a central circular region that matched the geometry of an IgG spot. The strength of the barrier was parameterized by $p_{\text{exclusion}}$ –the probability that a particle colliding with the barrier is unable to breach it and enter the enclosed region. A diffusion coefficient of 0.053 $\mu m^2/s$ was used for the simulation, to match the value measured experimentally (Fig. 1E). As expected, increasing the exclusion probability reduced access to the enclosed region (Fig. 2A). When compared at 20 s, the time period of our SMT experiments, the observed ratio of particle densities inside the barrier to outside was most consistent with simulation results for $p_{\text{exclusion}} > 0.5$ (Fig. 2B).

Since observed trajectories deviate from Brownian diffusion and have variable track lengths (Fig. 2C), we additionally used a statistical bootstrap approach to match simulated tracks more closely with observed tracks. This more robust analysis confirmed that observed trajectories are most consistent with a non-zero exclusion probability ($p_{\text{exclusion}} \approx 0.75$, Fig. 2D). We also estimated the fraction of its lifetime that a randomly chosen trajectory would spend inside the barrier (Fig. 2E). The observed distribution clearly deviated from bootstrap distributions for no/low exclusion probabilities. Together, these results support the existence of a diffusional barrier that restricts the entry of CD45 into regions of ligand engagement.

While the depletion of CD45 from sites of frustrated phagocytosis is consistent with the establishment of a diffusion barrier, it was conceivable that the phosphatase was cleared from these areas by increased focal exocytosis of endomembranes devoid of CD45 or by selective endocytosis. However, neither Dectin-1 (a glucan receptor) nor CD36 (a type B scavenger receptor) were excluded from the sites of engagement (Figs. S2G–H), implying that a generalized displacement of membrane proteins was not occurring. Also, CD45 was very often observed to accumulate around the areas of depletion (e.g. Fig. 4A,H), consistent with lateral displacement and arguing against selective endocytosis. These observations favor a diffusional barrier as the simplest mechanism responsible for CD45 exclusion.

The area of depletion of CD45 extends beyond regions of microclustered Fcγ receptors

The kinetic segregation model developed in lymphoid cells postulates that exclusion of phosphatases relies on the congregation of receptors first into microclusters, then in a larger consolidated structure, the cSMAC (Varma et al., 2006). To assess whether similar structures are generated during phagocytosis, we analyzed the distribution of FcγRIIA-GFP during frustrated phagocytosis. As shown in Fig. 3A, the receptors aggregated into discrete microclusters, despite the fact that the ligand was distributed homogeneously on the surface of the coverslip. Of note, the microclusters failed to congregate into supermolecular structures like the cSMAC even after prolonged exposure (≥20 min) to the target surface. Strikingly, while the microclustered receptors occupied less than 25% of the frustrated phagosomal surface, CD45 was excluded from the entire contact area (Fig. 3A). It was nevertheless possible that receptors present at a lower density –insufficient to form visible microclusters– associate with the immobilized IgG and occupy the remainder of the contact zone, contributing to exclude CD45.

To better define the relationship between the area occupied by engaged receptors and that where CD45 is excluded, we used micropatterning. In cells deposited on micropatterned coverslips, Fcγ receptors clustered only in areas where IgG was printed (Figs. 3B and S3) resulting in focal activation, detectable as phosphotyrosine accumulation (Fig. 3C). F-actin was found to accumulate in the vicinity of the micropatterned ligand (Figs. 3B and 4G). Remarkably, while receptor clustering was strictly confined to the area where the ligand was deposited (Figs. 3B and S3; quantified in 3H), phosphotyrosine and especially actin were found also in the surrounding area.

As illustrated in Fig. 3D, the area of depletion of CD45 clearly exceeded the spot where the ligand was micropatterned, i.e. the zone of receptor engagement. The diameter of the CD45 depletion zone, which was nearly twice that of the zone of receptor-ligand complex formation, coincided with the region of F-actin accumulation (Fig. 3H), suggesting that the cytoskeleton contributes to the establishment of the diffusion barrier. It was therefore important to define how actin is anchored to the plasmalemma in the area that demarcates the zone of depletion. Integrins, which are activated upon Fcγ receptor engagement (Jones et al., 1998), seemed an attractive candidate. Indeed, both active integrins (Fig. 3G) and the associated actin-binding protein vinculin (Fig. 3F) were enriched beyond the micropatterned IgG, intimately associated with the actin cytoskeleton in a comparable area (Fig. 3H). Similar results were obtained whether the area surrounding the micropattern was coated with fibrinogen (Fig. S2A,B) or fibronectin (Fig. S2D,E), or left uncoated (Fig. 3). The zone of integrin activation and vinculin recruitment delimited the CD45 depletion zone not only in the frustrated phagocytosis model (Fig. 3D–G; Video 1), but also in *bona fide* 3-dimensional phagocytosis (Fig. 3I–J).

How are integrins activated at a distance from the site of receptor activation? A diffusible second messenger may mediate the expansion of the signal beyond the micropatterned zone. We tested this notion using the PH domain of Akt. As reported (Marshall et al., 2001), 3'-polyphosphoinositides are generated by the activated Fcγ receptors and, importantly, diffuse

away from the sites of receptor stimulation, generating a halo (Fig. 3E) with a diameter that closely matches the region of actin polymerization and CD45 depletion (Fig. 3H).

Integrin activation and actin polymerization are required for CD45 removal

The preceding observations suggest that integrins are involved in generating the diffusional barrier that excludes CD45. This was tested by deactivating the integrins after depletion of the phosphatases had occurred. When integrins were acutely inactivated by removal of divalent cations with EDTA, CD45 rapidly re-entered the area where actin had polymerized around active receptors, and was only partially excluded from the receptor-ligand interaction zone (Fig. 4A). Note that, following integrin deactivation, the cells retracted and remained adherent to the coverslip only at sites of Fcγ receptor engagement. Partial disassembly of actin using latrunculin also enabled CD45 to re-enter the contact zones (Fig. 4A–B). These observations were validated by SMT: while under control conditions CD45 molecules were unable to enter the perimeter of the receptor engagement zone, they readily did so following actin disassembly or integrin deactivation (Fig. 4D). It is noteworthy that re-entry of the phosphatases into the micropatterned zone was accompanied by a marked reduction in phosphotyrosine accumulation in that area (Fig. 4C). Neither latrunculin nor EDTA treatment altered the stability of the Fcγ receptor-IgG complexes, as measured by FRAP (Fig. S3B).

Because divalent cation chelation can have other effects, we impaired inside-out activation of integrins and their linkage to F-actin by alternative, more selective means. The engagement of Fc receptors leads to stimulation of CalDAG-GEF1, a GEF for Rap (Stolla et al., 2011). Activation of Rap is essential for inside-out activation of integrins (Gloerich and Bos, 2011). We isolated macrophages from CalDAG-GEF1$^{-/-}$ mice and assessed their barrier function during phagocytosis (Fig. 4E). Unlike wild-type bone marrow-derived cells, CalDAG-GEF1-deficient macrophages failed to generate an expansive CD45 depletion zone (Fig. 4F). Failure to activate the integrins from the inside was in all likelihood responsible for this observation. Accordingly, when plated onto micropatterned IgG, CalDAG-GEF1-deficient macrophages did not form the organized concentric rings of vinculin, indicative of integrin activation, which were observed in their wildtype counterparts (Fig. 4G). The inability of CalDAG-GEF1$^{-/-}$ macrophages to form an integrin-based barrier and exclude CD45 was also associated with decreased phosphotyrosine accumulation at sites of attachment (Fig S3D).

The involvement of integrins in CD45 exclusion was also demonstrated by expressing a truncated form of talin that prevents their association to vinculin and actin (Zhang et al., 2008). When macrophages expressing this construct were plated on coverslips fully coated with IgG, CD45 freely traversed the contact zone, which failed to assemble the actin belt normally formed around the periphery of frustrated phagosomes (Fig. S3E).

Formation of Fcγ receptor-induced active integrin structures was dependent on Arp2/3 but independent of formins, myosin II and microtubules, and depletion of CD45 followed the same pattern (Fig. 4H–I). Our data are therefore consistent with a model where Fcγ receptors remotely activate integrins that link to Arp2/3-generated actin filaments via talin and vinculin, thereby cementing a diffusional barrier that precludes entry of CD45 (Fig. 4J).

Macrophage podosomes exclude CD45

The peri-receptor actin complexes bear resemblance to podosomes; this prompted us to test whether the latter structures similarly exclude CD45. We used structured illumination microscopy (SIM) to visualize podosomes on the ventral membrane of cells grown on coverslips in the presence of serum, but otherwise unstimulated. Podosomes were identified as having phosphotyrosine and F-actin-rich cores surrounded by vinculin rings (Fig. S4A). When visualized by immunostaining, CD45 was indeed excluded from podosomes, removed from their signaling cores (Fig. S4B). Tracking of single CD45 molecules on the ventral membrane revealed that as they approached podosomes the phosphatases were redirected around them, never entering their core (Fig. S4C). These data demonstrate that regions where integrins bind to the substratum are seemingly sufficient to exclude CD45.

Size-dependent exclusion of the ectodomain of CD45

Our observation that integrins and F-actin are critical for exclusion of CD45 raises the possibility that the cytosolic tail and/or the transmembrane domain of CD45 may be required for segregation. To assess the mode of exclusion we used synthetic glycopolymers of defined sizes. These glycopolymers consist of repeating units of alpha N-acetyl galactosamine that mimic the physical bulk of a glycoprotein's ectodomain. A dipalmitoylated terminus allows insertion into the outer leaflet of the plasma membrane (Fig. 5A), but unlike CD45 the glycopolymers lack transmembrane and cytoplasmic domains. As such, they should be unimpeded by intracellular diffusional barriers. One such glycopolymer mimetic (glycomimetic) that extends ≈80 nm perpendicular to the plane of the membrane was excluded from the area around micropatterned IgG, as observed for CD45 (Fig. 5B). SMT confirmed that, like CD45, this long glycomimetic diffuses freely along the outer leaflet of the membrane, yet is deflected away from areas surrounding the micropatterned opsonin (Fig. 5C). The exclusion requires active integrins and an intact actin skeleton, because the glycomimetic was able to enter the receptor engagement area when EDTA or latrunculin were present (Fig. 5C). By contrast, a short (3 nm) glycomimetic – shorter than the ectodomains of integrins– was not excluded from the contact areas. These data support the idea that CD45 is physically excluded by the apposition of the phagocyte membrane to its target by an integrin- and actin-dependent mechanism.

CD45 depletion is required for phagocytosis

While CD45 and CD148 are unquestionably excluded from the phagocytic cup (Goodridge et al., 2011; see also Figs. 1–3), it remains to be established whether this event is in fact essential for successful phagocytosis. We performed ectodomain swapping experiments to assess this requirement. Constructs consisting of the transmembrane and cytosolic domains of CD45 were fused to either the ectodomain of CD43 –a long (≈45 nm) molecule of dimensions similar to CD45– or that of CD2 –a much shorter molecule (≤7 nm; Fig. 5A). As shown in Figs. 5D and S4D, when expressed in either HeLa or RAW264.7 cells the longer chimeric construct (CD43–CD45) was excluded from areas where cells attached to the substratum via integrins, while the shorter (CD2–CD45) chimera was not. More importantly, while expression of the CD43–CD45 chimera was without effect on phagocytosis, the short CD2–CD45 chimera markedly inhibited phagocytic efficiency (Fig. 5E–F). This was

dependent on the phosphatase activity of the construct (Fig. 5E–F). Our data suggest that depletion of CD45/CD148, which requires their long extracellular domain, is key to the completion of phagocytosis.

Integrins facilitate engagement of distant points of opsonization

Phagocytosis is conceived to proceed by a zipper-like mechanism whereby receptors drive particle engulfment by serially binding to ligands on the target surface. This concept, which requires a high density of ligands, was derived from experimental models where phagocytosis was optimized by coating particles heavily with opsonins (Griffin et al., 1975). In nature, however, opsonization is less likely to result in homogeneous coverage of the target particle. We propose that, by activating surrounding integrins, opsonic receptors like Fcγ facilitate bridging between sparse specific ligands. The high ligand promiscuity of integrins would confer efficiency to the phagocytic process. To test this hypothesis, we micropatterned glass with IgG and compared the ability of macrophages to engage Fcγ receptors under conditions where integrins were able to associate with the remaining (IgG-devoid) surface, or were prevented from doing so by coating the glass with polyethylene glycol (PEG). Visualization of Fcγ receptors in the plane of contact by either SIM (Fig. 6A) or TIRF revealed that extensions of the membrane containing unoccupied Fcγ receptors were routinely observed beyond the regions of micropatterned IgG, but only when integrins were allowed to engage the surrounding substrate. Such extensions were facilitated by the activation of integrins and associated polymerization of actin generated by receptor activation: only small amounts of F-actin were detected in association with the receptor-ligand complexes when integrin engagement was precluded by PEG, and the actin was confined to the IgG spots (Fig. 6B).

The bridging effect of integrins, defined as their ability to multiply the number of receptor engagement sites, is quantified in Fig. 6C. Of note, the contribution of the integrins is more significant when the distance between opsonin spots is greater.

Integrins coordinate the phagocytic response

Even when confronted with a surface homogeneously coated with ligands, Fcγ receptors form microclusters that cover only a fraction of the phagocytic cup (Figs. 3A,7A). Because the ligands are immobile, larger entities such as the cSMAC cannot form. How, then, is the phagocytic response coordinated? It is noteworthy that, despite the sparseness of microclusters, CD45 is excluded from the *entire* phagocytic cup, reflecting a unique mode of signal expansion and coordination. We postulate that activated integrins furnish the coordination required to exclude CD45 from the entire phagocytic cup. Indeed, when macrophages already having undergone frustrated phagocytosis were treated with EDTA to reverse integrin activation, single CD45 molecules reentered the depletion zone (Fig. 7A). Interestingly, the CD45 molecules avoid the receptor microclusters –resembling observations made during early stages of formation of immunological synapses (James and Vale, 2012)– but they appear to diffuse freely between them. This implies that the phagosomal membrane is tightly apposed to the target in its entirety only when the integrins are active and able to engage their ligands.

The preceding observations suggest that integrins serve as a coordinator of the effects of sparse receptor microclusters which, unlike those of lymphoid cells, are unable to coalesce by lateral diffusion into larger structures. To test this we analyzed the distribution of CD45 on micropatterned coverslips where the distance between opsonin spots was varied. When the IgG-coated zones are 6 μm apart, macrophages exclude CD45 from the area surrounding each spot. Bringing the spots closer together results in partial overlap and ultimately coalescence of the individual depletion areas, resulting in extensive depletion resembling that generated by a homogeneously coated surface. Thus, when the distance between contact sites reaches a defined threshold, the cells "sense" the unevenly coated surface as a single target. Remarkably, the threshold distance (≈2 μm) is identical to the radius of activation of integrins around the activated receptors (Fig. 3).

The depletion of CD45 from a large area when the micropatterned spots were sufficiently close (2 μm) enabled the cells to coordinate the effectors leading to the phagocytic response. An external belt of actin was detected in these cells, with a large area of clearance in the middle, resembling the pattern observed during frustrated phagocytosis of homogeneously coated surfaces (Fig. 7C) and also during 3-dimensional phagocytosis. By contrast, on micropatterns where the areas between IgG spots were blocked by PEG, not only was the overall contact area smaller, but the distribution of actin was different, with little clearance in the center. Thus, expansion of the phagocytic cup and clearance of actin at its base – which is required for successful engulfment of large targets (Araki et al., 1996; Cox et al., 1999)– needs engagement of integrins activated by the receptors.

The preceding data imply that the dependence on integrin activation will vary with the spatial distribution and density of phagocytic ligands. To verify whether these predictions apply to physiological, 3-dimensional phagocytosis, we studied the integrin dependence of phagocytosis of *Salmonella* typhimurium ΔinvA SL1344. Because it lacks the invA protein, this strain is unable to invade host cells and must be taken up by phagocytosis (Fig. 7D). *Salmonella* expresses O antigens on its wall, and H antigens in flagella. We took advantage of these spatially segregated antigens by opsonizing the bacteria with H antiserum, O antiserum, or both, without changing the total concentration of IgG. The role of integrins was assessed in two independent ways: by omission of divalent cations, or by preventing engagement using a mixture of blocking antibodies to β1 and β2 integrins. When the bacteria were opsonized with both antisera, macrophages did not require integrins to complete phagocytosis (Fig. 7E). Bacteria opsonized with combined O and H sera did not require CalDAG-GEF1 either (Fig. 7F). In stark contrast, bacteria opsonized with only one of the antisera required integrins and CalDAG-GEF1 for optimal phagocytosis (Fig. 7E–G). Partially opsonized *Salmonella* (i.e. exposed to only one of the antisera) were very often incompletely ingested by cells with inactivated integrins (Fig. 7G). Indeed, the unopsonized regions of bacteria remained outside the macrophages, suggesting that the phagocytes could not coordinate distant points of attachment to internalize the entire pathogen.

We also tested phagocytic efficiency while varying the concentration of IgG. As anticipated, phagocytosis increased and eventually saturated as the titer of the opsonin increased (Fig. 7H). It is noteworthy that inactivation of integrins with EDTA was without effect at the highest opsonin concentrations, but exerted a progressively greater inhibitory effect as the

titer was reduced. Conversely, preactivation of integrins by addition of phorbol myristoyl acetate (PMA) enhanced phagocytic efficiency when the ligand titer was low, but was similarly without effect at saturating concentrations of opsonin (Fig. 7H). That the effect of EDTA was caused by inactivation of integrins was verified using the inhibitory truncated form of talin. At subsaturating concentrations of opsonin, the talin head domain markedly reduced phagocytic efficiency (Fig. 7I). Together, our findings indicate that integrins determine the effectiveness of the phagocytic response, lowering the threshold of opsonization required for effective engulfment.

Discussion

We report that removal of phosphatases from the phagocytic cup is essential for completion of phagocytosis. It is noteworthy that exclusion of CD45/CD148 need not be complete; phosphatase activity in the activation zone must only decrease below the rate of SFK phosphorylation to result in net accumulation of phosphorylated proteins and the associated activation.

While the intrinsic motion of CD45 is passive and random (Brownian), its directional exclusion is mediated by an expanding diffusional barrier that requires active integrins and an intact actin cytoskeleton. The rapid centrifugal displacement of the phosphatases is facilitated by the marked increase in their mobility noted upon immunoreceptor engagement: the fraction of confined CD45 molecules decreased and the size of the remaining confinement zones increased. These effects combined to greatly increase the overall diffusion coefficient. The behavior elicited by phagocytic receptors differs diametrically from that reported in lymphoid cells, where CD45 mobility *decreases* upon activation (Cairo et al., 2010; Drbal et al., 2007).

Whereas in lymphocytes the immunoreceptors themselves are believed to exclude the phosphatases, the area of CD45 depletion in phagocytes extends well beyond the microclusters formed by the receptors. A surrounding area of depletion is delimited by integrins, which are activated downstream of the phagocytic receptors, and displays elevated levels of phosphatidylinositol 3,4,5-*tris*phosphate. Inside-out activation of integrins requires conversion of GDP-Rap1 to its GTP-bound form, a process catalyzed by the diacylglycerol-stimulated exchange factor CalDAG-GEF1 (Kawasaki et al., 1998). Because phosphatidylinositol 3,4,5-*tris*phosphate activates the phospholipases that generate diacylglycerol, and because we have shown the latter to accumulate at sites of Fcγ receptor-mediated phagocytosis (Marshall et al., 2001), we conclude that the zone of CD45 depletion expands beyond the region of receptor engagement via formation and lateral diffusion of lipid second messengers. Indeed, macrophages from CalDAG-GEF1 null mice failed to form integrin barriers for CD45. It is conceivable that phosphatase exclusion in lymphoid cells utilizes a similar process. In fact, in the T cell immunological synapse CD45 density was noted to be low within regions of LFA-1/ICAM engagement (Johnson et al, 2000), and invadosome/podosome-like structures were reported to form between T cells and antigen-presenting cells (Sage et al, 2012).

Activation of integrins in the area surrounding active receptors serves 2 purposes. First, by latching onto the target particle, the activated integrins bridge the space between Fcγ receptor ligands, a critical event in the development of the phagocytic cup, particularly when the targets are sparsely opsonized (Fig. 7). In this regard, it is important to bear in mind that whereas Fcγ receptors bind only the Fc portion of IgG, active integrins can associate with a plethora of ligands (Fig. S5) including native- or modified-self molecules, as well as non-self (i.e. microbial pathogen) components (Boehm and DeNardin, 2008; Yakubenko et al., 2002). Thus, we envisage Fcγ receptors as conferring specificity to the phagocytic event, while the more promiscuous integrins increase the avidity and efficiency of the process. Secondly, by expanding the area of depletion of the phosphatases, the integrins coordinate (integrate) the phagocytic response. This was most apparent when the distance between micropatterned spots was varied: it was only when the width of the integrin halo around the ligand spots matched half the distance between spots that the area of CD45 depletion consolidated into a single large zone, as observed in physiological conditions (Fig. 7B).

While differences exist between the phagocytic and lymphoid responses, the depletion of CD45 in both cases relies, at least in part, on the physical exclusion of its long extracellular domain, which was recently shown to be rigid by the elegant studies of Chang et al. (in press). This was validated using synthetic glycomimetics (Fig. 5A–C), as well as chimeric phosphatase constructs (Fig. 5D,E). In the case of phagocytic cells, however, the exclusion requires and is likely effected by integrins. Though somewhat longer than the Fcγ receptors, the integrins are nevertheless considerably shorter than even the shortest splice variant of CD45; the latter is estimated to extend ≈30 nm, while the bent and extended forms of integrins reach only 11 nm and 19 nm, respectively (Ye et al., 2010). The heterologous expression experiments of Fig. 5D, as well as the observations made on adherent macrophages (Fig. S4), suggest that integrins suffice to exclude CD45, so that the process is not restricted to immunoreceptor-mediated activation. Therefore, displacement of transmembrane phosphatases away from areas of integrin engagement may also be instrumental in the formation of podosomes and in the generation of sealing zones where osteoclasts perform bone resorption.

Size-based exclusion of CD45/CD148 may not be the only mechanism underlying their displacement from the phagocytic cup. The phosphatases are major constituents of the glycocalyx, raising the possibility that their displacement may be coordinated with that of other glycoproteins. In preliminary experiments, however, we found no evidence that CD45 exclusion depends on glycocalyx interconnectivity; disruption of the galectin lattice did not prevent exclusion of the phosphatase (Fig. S3F). Nevertheless, an ensemble, mechanical movement of the glycocalyx may be important to exclude other molecules. We similarly failed to find any evidence that CD45 is displaced by extracellular DNA, which is extruded from some activated phagocytes by a process (NETosis) dependent on activation of NOX2; we did not detect extracellular DNA during phagocytosis, nor could we prevent the displacement of CD45 by inhibiting NOX2 (Fig. S3F). Lastly, we considered whether CD45 might be shed by proteases. CD45 depletion persisted despite inhibition of metalloproteases using the broad-spectrum antagonist Marimastat (Fig. S3F). Thus, physical extrusion of CD45 by tight membrane apposition remains the simplest mechanism to account for its depletion, though additional mechanisms cannot be discounted.

Because displacement of the phosphatases seems to depend on the physical exclusion of their extracellular domain from the narrow junction formed by the tight apposition of the membrane and the phagocytic target, the requirement for actin –a cytosolic protein– would appear surprising. However, there is clear evidence that linkage to the actin skeleton stabilizes the active (extended) form of integrins (Zhu et al., 2008a). Nevertheless, it is conceivable that actin contributes to the formation of a diffusional barrier in other ways as well. There is evidence for the existence of a barrier that limits the mobility of lipids and membrane-tethered proteins during the course of phagocytosis (Golebiewska et al., 2011) and even during macropinocytosis (Yoshida et al., 2009), where the physical exclusion model proposed for CD45 would not apply.

In summary we have described the sequence of events that lead to phosphatase exclusion and enable SFK activation and the consequent phagocytic response. We found that opsonic receptors trigger a remote wave of integrin activation that serves to bridge distant ligands, fixing what would appear to be a broken zipper, and integrating the response of multiple immobile microclusters, obviating the need for them to coalesce into larger structures, as reported in lymphoid cells.

Materials and methods

Cell isolation and culture

Primary macrophages were derived from monocytes isolated from heparinized blood of human donors. Peripheral Blood mononuclear cells were isolated using Lympholyte-H (Cedarlane), resuspended in DMEM and seeded onto TC plastic dishes for 30 min to select adherent cells. Non-adherent cells were removed by washing with DMEM and adherent cells were then incubated in DMEM with L-glutamine containing 10% heat-inactivated serum, 100 U/mL penicillin, 100 μg/mL streptomycin and 10 ng/mL hM-CSF (Peprotech Inc.) for 5–7 days. To isolate murine macrophages, we harvested the marrow of femoral bones from 6–8 week old C57Bl/6 wildtype or CalDAG-GEF1-null mice (Bergmeier et al., 2007). Cells were washed before culturing in DMEM with L-glutamine and 10% heat-inactivated serum and 100 U/mL penicillin, 100 μg/mL streptomycin, and 10 ng/mL mM-CSF (Peprotech Inc.) for 5–7 days. Parental and mCherry-actin-expressing RAW 264.7 cells were cultured as described (Bohdanowicz et al., 2010).

Single-particle labeling and tracking of CD45

To label single CD45 molecules, cells were washed with HBSS, then incubated with 100 ng/mL of Cy3-, Cy3B- or biotin-conjugated anti-CD45 Fab fragments for 5 min. Cells labeled with biotinylated Fabs were washed in cold PBS, then incubated with streptavidin-655 Qdots (1:10,000 dilution) for 5 min at 4°C, to minimize lateral mobility and clustering, then washed with complete DMEM containing excess biotin to block unoccupied avidin sites and prevent cross-linking. Cells labeled with Cy3B-conjugated Fab fragments were washed in PBS at 25°C. Cells were mechanically lifted in complete DMEM at 37°C before being laid over coverslips that were micropatterned or homogeneously coated with IgG. Single cells were imaged on a Zeiss Axiovert 200M microscope, equipped with a 100× NA 1.45 oil objective, a custom 2.4× magnification lens, and a back-thinned EM-CCD

camera (Hamamatsu). For Qdot-labeled particles, acquisitions were performed at 33 Hz. For Cy3B-labeled particles, acquisitions were at 10 Hz. Single particles were detected and tracked as described (Jaqaman et al., 2008). Motion types and diffusion coefficients were determined using a moment scaling spectrum (MSS) analysis, as described (Jaqaman et al., 2011). The dimensions of the confinement zones were derived by eigenvalue decomposition of the variance-covariance matrix of particle positions.

Supplementary Material

Refer to Web version on PubMed Central for supplementary material.

ACKNOWLEDGMENTS

S.A.F. is funded by a fellowship from the Heart and Stroke Foundation of Canada. Work supported by grant FDN 143202 from the Canadian Institutes of Health Research.

References

Araki N, Johnson MT, Swanson JA. A role for phosphoinositide 3-kinase in the completion of macropinocytosis and phagocytosis by macrophages. The Journal of cell biology. 1996; 135:1249–1260. [PubMed: 8947549]

Batista FD, Iber D, Neuberger MS. B cells acquire antigen from target cells after synapse formation. Nature. 2001; 411:489–494. [PubMed: 11373683]

Bergmeier W, Goerge T, Wang HW, Crittenden JR, Baldwin AC, Cifuni SM, Housman DE, Graybiel AM, Wagner DD. Mice lacking the signaling molecule CalDAG-GEFI represent a model for leukocyte adhesion deficiency type III. The Journal of clinical investigation. 2007; 117:1699–1707. [PubMed: 17492052]

Boehm TK, DeNardin E. Fibrinogen binds IgG antibody and enhances IgG-mediated phagocytosis. Human antibodies. 2008; 17:45–56. [PubMed: 19029661]

Bohdanowicz M, Cosio G, Backer JM, Grinstein S. Class I and class III phosphoinositide 3-kinases are required for actin polymerization that propels phagosomes. The Journal of cell biology. 2010; 191:999–1012. [PubMed: 21115805]

Botelho RJ, Harrison RE, Stone JC, Hancock JF, Philips MR, Jongstra-Bilen J, Mason D, Plumb J, Gold MR, Grinstein S. Localized diacylglycerol-dependent stimulation of Ras and Rap1 during phagocytosis. The Journal of biological chemistry. 2009; 284:28522–28532. [PubMed: 19700408]

Botelho RJ, Teruel M, Dierckman R, Anderson R, Wells A, York JD, Meyer T, Grinstein S. Localized biphasic changes in phosphatidylinositol-4,5-bisphosphate at sites of phagocytosis. The Journal of cell biology. 2000; 151:1353–1368. [PubMed: 11134066]

Cairo CW, Das R, Albohy A, Baca QJ, Pradhan D, Morrow JS, Coombs D, Golan DE. Dynamic regulation of CD45 lateral mobility by the spectrin-ankyrin cytoskeleton of T cells. The Journal of biological chemistry. 2010; 285:11392–11401. [PubMed: 20164196]

Chang VT, Fernandes R, Ganzinger KA, Lee SF, Siebold C, McColl J, Jönsson P, Palayret M, Harlos K, Coles CH, Jones EY, Lui Y, Huang E, Gilbert RJC, Klenerman D, Aricescu AR, Davis SJ. CD45 segregation at “close-contacts” initiates T-cell receptor signaling. Nature immunology. (in press).

Cordoba SP, Choudhuri K, Zhang H, Bridge M, Basat AB, Dustin ML, van der Merwe PA. The large ectodomains of CD45 and CD148 regulate their segregation from and inhibition of ligated T-cell receptor. Blood. 2013; 121:4295–4302. [PubMed: 23580664]

Cox D, Tseng CC, Bjekic G, Greenberg S. A requirement for phosphatidylinositol 3-kinase in pseudopod extension. The Journal of biological chemistry. 1999; 274:1240–1247. [PubMed: 9880492]

Davis SJ, van der Merwe PA. The kinetic-segregation model: TCR triggering and beyond. Nature immunology. 2006; 7:803–809. [PubMed: 16855606]

Drbal K, Moertelmaier M, Holzhauser C, Muhammad A, Fuertbauer E, Howorka S, Hinterberger M, Stockinger H, Schutz GJ. Single-molecule microscopy reveals heterogeneous dynamics of lipid raft components upon TCR engagement. International immunology. 2007; 19:675–684. [PubMed: 17446208]

Evans JG, Correia I, Krasavina O, Watson N, Matsudaira P. Macrophage podosomes assemble at the leading lamella by growth and fragmentation. The Journal of cell biology. 2003; 161:697–705. [PubMed: 12756237]

Flannagan RS, Jaumouille V, Grinstein S. The cell biology of phagocytosis. Annual review of pathology. 2012; 7:61–98.

Gloerich M, Bos JL. Regulating Rap small G-proteins in time and space. Trends in cell biology. 2011; 21:615–623. [PubMed: 21820312]

Golebiewska U, Kay JG, Masters T, Grinstein S, Im W, Pastor RW, Scarlata S, McLaughlin S. Evidence for a fence that impedes the diffusion of phosphatidylinositol 4,5-bisphosphate out of the forming phagosomes of macrophages. Molecular biology of the cell. 2011; 22:3498–3507. [PubMed: 21795401]

Goodridge HS, Reyes CN, Becker CA, Katsumoto TR, Ma J, Wolf AJ, Bose N, Chan AS, Magee AS, Danielson ME, et al. Activation of the innate immune receptor Dectin-1 upon formation of a 'phagocytic synapse'. Nature. 2011; 472:471–475. [PubMed: 21525931]

Grakoui A, Bromley SK, Sumen C, Davis MM, Shaw AS, Allen PM, Dustin ML. The immunological synapse: a molecular machine controlling T cell activation. Science. 1999; 285:221–227. [PubMed: 10398592]

Griffin FM Jr, Griffin JA, Leider JE, Silverstein SC. Studies on the mechanism of phagocytosis. I. Requirements for circumferential attachment of particle-bound ligands to specific receptors on the macrophage plasma membrane. The Journal of experimental medicine. 1975; 142:1263–1282. [PubMed: 1194852]

Hermiston ML, Zikherman J, Zhu JW. CD45, CD148, and Lyp/Pep: critical phosphatases regulating Src family kinase signaling networks in immune cells. Immunological reviews. 2009; 228:288–311. [PubMed: 19290935]

James JR, Vale RD. Biophysical mechanism of T-cell receptor triggering in a reconstituted system. Nature. 2012; 487:64–69. [PubMed: 22763440]

Jaqaman K, Kuwata H, Touret N, Collins R, Trimble WS, Danuser G, Grinstein S. Cytoskeletal control of CD36 diffusion promotes its receptor and signaling function. Cell. 2011; 146:593–606. [PubMed: 21854984]

Jaqaman K, Loerke D, Mettlen M, Kuwata H, Grinstein S, Schmid SL, Danuser G. Robust single-particle tracking in live-cell time-lapse sequences. Nature methods. 2008; 5:695–702. [PubMed: 18641657]

Jaumouille V, Jaqaman K, Das R, Lowell CA, Grinstein S. Actin cytoskeleton reorganization by syk regulates Fc receptor responsiveness by increasing its lateral mobility and clustering. Developmental cell. 2014

Jones SL, Knaus UG, Bokoch GM, Brown EJ. Two signaling mechanisms for activation of αM β2 avidity in polymorphonuclear neutrophils. The Journal of biological chemistry. 1998; 273:10556–10566. [PubMed: 9553116]

Kawasaki H, Springett GM, Toki S, Canales JJ, Harlan P, Blumenstiel JP, Chen EJ, Bany IA, Mochizuki N, Ashbacher A, et al. A Rap guanine nucleotide exchange factor enriched highly in the basal ganglia. Proceedings of the National Academy of Sciences. 1998; 95:13278–13283.

Marshall JG, Booth JW, Stambolic V, Mak T, Balla T, Schreiber AD, Meyer T, Grinstein S. Restricted accumulation of phosphatidylinositol 3-kinase products in a plasmalemmal subdomain during Fc receptor-mediated phagocytosis. The Journal of cell biology. 2001; 153:1369–1380. [PubMed: 11425868]

Monks CR, Freiberg BA, Kupfer H, Sciaky N, Kupfer A. Three-dimensional segregation of supramolecular activation clusters in T cells. Nature. 1998; 395:82–86. [PubMed: 9738502]

Paszek MJ, DuFort CC, Rossier O, Bainer R, Mouw JK, Godula K, Hudak JE, Lakins JN, Wijekoon AC, Cassereau L, et al. The cancer glycocalyx mechanically primes integrin-mediated growth and survival. Nature. 2014; 511:319–325. [PubMed: 25030168]

Stolla M, Stefanini L, Andre P, Ouellette TD, Reilly MP, McKenzie SE, Bergmeier W. CalDAG-GEFI deficiency protects mice in a novel model of Fc RIIA-mediated thrombosis and thrombocytopenia. Blood. 2011; 118:1113–1120. [PubMed: 21652673]

Torres AJ, Vasudevan L, Holowka D, Baird BA. Focal adhesion proteins connect IgE receptors to the cytoskeleton as revealed by micropatterned ligand arrays. Proceedings of the National Academy of Sciences. 2008; 105:17238–17244.

van der Merwe PA, Dushek O. Mechanisms for T cell receptor triggering. Nature reviews Immunology. 2011; 11:47–55.

Varma R, Campi G, Yokosuka T, Saito T, Dustin ML. T cell receptor-proximal signals are sustained in peripheral microclusters and terminated in the central supramolecular activation cluster. Immunity. 2006; 25:117–127. [PubMed: 16860761]

Yakubenko VP, Lishko VK, Lam SC, Ugarova TP. A molecular basis for integrin αM β2 ligand binding promiscuity. The Journal of biological chemistry. 2002; 277:48635–48642. [PubMed: 12377763]

Yamauchi S, Kawauchi K, Sawada Y. Myosin II-dependent exclusion of CD45 from the site of Fcgamma receptor activation during phagocytosis. FEBS letters. 2012; 586:3229–3235. [PubMed: 22771477]

Ye F, Hu G, Taylor D, Ratnikov B, Bobkov AA, McLean MA, Sligar SG, Taylor KA, Ginsberg MH. Recreation of the terminal events in physiological integrin activation. The Journal of cell biology. 2010; 188:157–173. [PubMed: 20048261]

Yoshida S, Hoppe AD, Araki N, Swanson JA. Sequential signaling in plasma-membrane domains during macropinosome formation in macrophages. Journal of cell science. 2009; 122:3250–3261. [PubMed: 19690049]

Zhang X, Jiang G, Cai Y, Monkley SJ, Critchley DR, Sheetz MP. Talin depletion reveals independence of initial cell spreading from integrin activation and traction. Nature cell biology. 2008; 10:1062–1068. [PubMed: 19160486]

Zhu J, Luo BH, Xiao T, Zhang C, Nishida N, Springer TA. Structure of a complete integrin ectodomain in a physiologic resting state and activation and deactivation by applied forces. Molecular cell. 2008a; 32:849–861. [PubMed: 19111664]

Zhu JW, Brdicka T, Katsumoto TR, Lin J, Weiss A. Structurally distinct phosphatases CD45 and CD148 both regulate B cell and macrophage immunoreceptor signaling. Immunity. 2008b; 28:183–196. [PubMed: 18249142]

Highlights

- Tyrosine phosphatases are excluded from sites of phagocytosis.
- An expanding diffusion barrier prevents phosphatase access to sites of phagocytosis
- Integrins activated by phagocytic receptors generate the diffusion barrier
- Activated integrins bridge sparse phagocytic receptors and coordinate phagocytosis

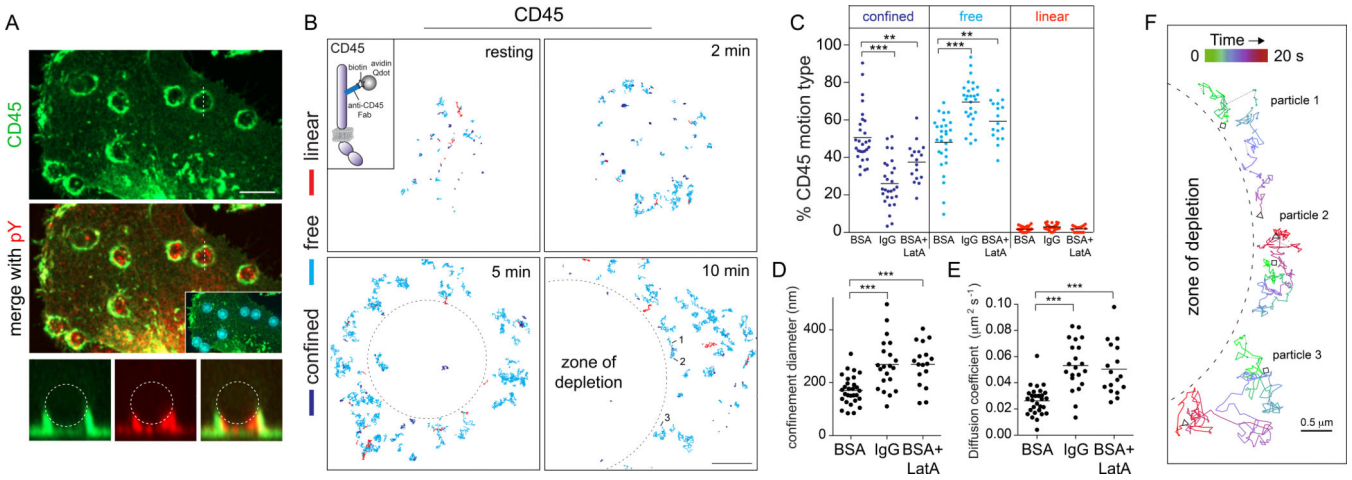

Fig. 1. CD45 is depleted from regions of contact between macrophages and IgG-opsonized targets by a diffusional barrier

A) Human macrophages incubated with polystyrene beads opsonized with 0.5 mg IgG/10^7 particles. Cells were fixed after 45 s and stained for CD45 (green), pY (red) and IgG (cyan, inset). Scale bar=10 μm. **B–F)** Single CD45 particles were visualized in macrophages using anti-CD45 Fab fragments labeled with Qdots (B, inset). **B)** Macrophages were seeded onto either BSA-coated or IgG-coated coverslips and particles tracked for 20 s at 33 Hz. CD45 trajectories were analyzed by MSS; the motion type for each trajectory is color-coded: confined (blue), free (cyan), or linear (red). Scale bar =5 μm. **C–E)** CD45 motion type (C), median confinement diameter (D) and median diffusion coefficient (E) for cells seeded on BSA (20 min), IgG (20 min), or BSA + LatA (15+5 min) were determined from 10 s recordings. Horizontal lines are means of ≥17 cells from 3 independent experiments; >1000 trajectories analyzed/condition. **F)** Three trajectories from (B) shown with color-coded time course. Depletion zones drawn in B and F delineate the area depleted of CD45. They were drawn to approximate the contour of the F-actin ring.

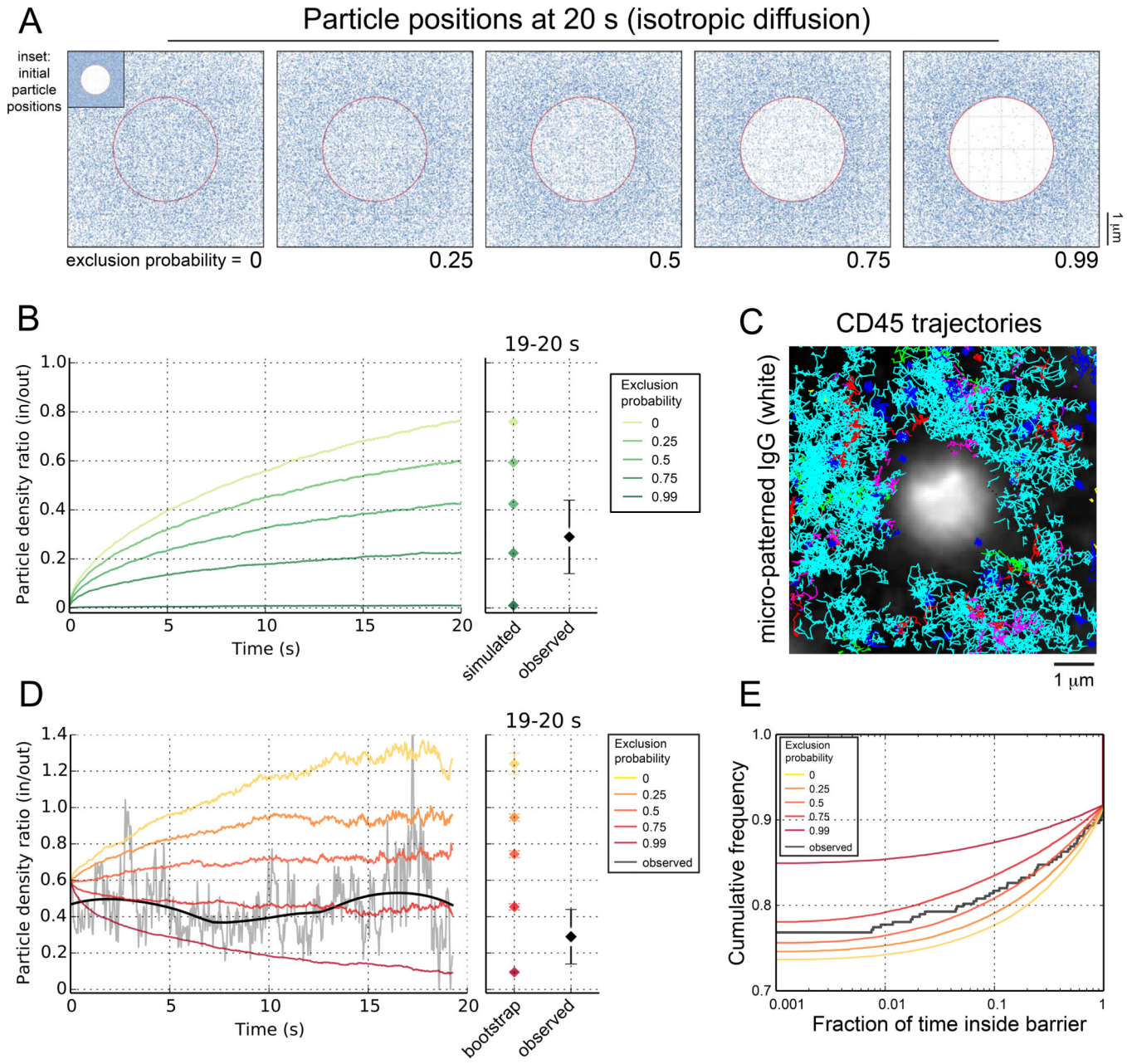

Fig. 2. Quantifying CD45 exclusion from sites of receptor engagement

A) Initial and final positions of simulated particles undergoing Brownian diffusion in the presence of a barrier. Particles were initially dispersed randomly outside a circular region of radius 1.6 μm centered in a square with 6 μm sides (inset). The circular region is enclosed by a barrier (shown in red) characterized by $p_{\text{exclusion}}$ –the probability that a particle colliding with the barrier will be unable to breach it. Particle positions at 20 s are shown for different exclusion probabilities. **B**) Ratio of density of particles inside/outside the barrier as a function of time for the 20 s simulation period (left), and the values calculated for the last 1 s of simulated and observed tracks (right). **C**) Single CD45 molecules were tracked for 20 s in the vicinity of micropatterned IgG. Image shows the superposition of 10 micropatterns from

a single experiment. 300 trajectories are shown, averaging 86 frames each. **D**) Time course and asymptotic values of particle density ratios for bootstrap trajectories generated using different exclusion probabilities (color-coded) and for observed CD45 tracks (gray trace + black trend line). >300 observed CD45 tracks from the vicinity of 18 antigen spots were pooled to generate the experimental time course. **E**) Observed and bootstrap distributions of the fraction of time a random trajectory spends inside the barrier for different exclusion probabilities.

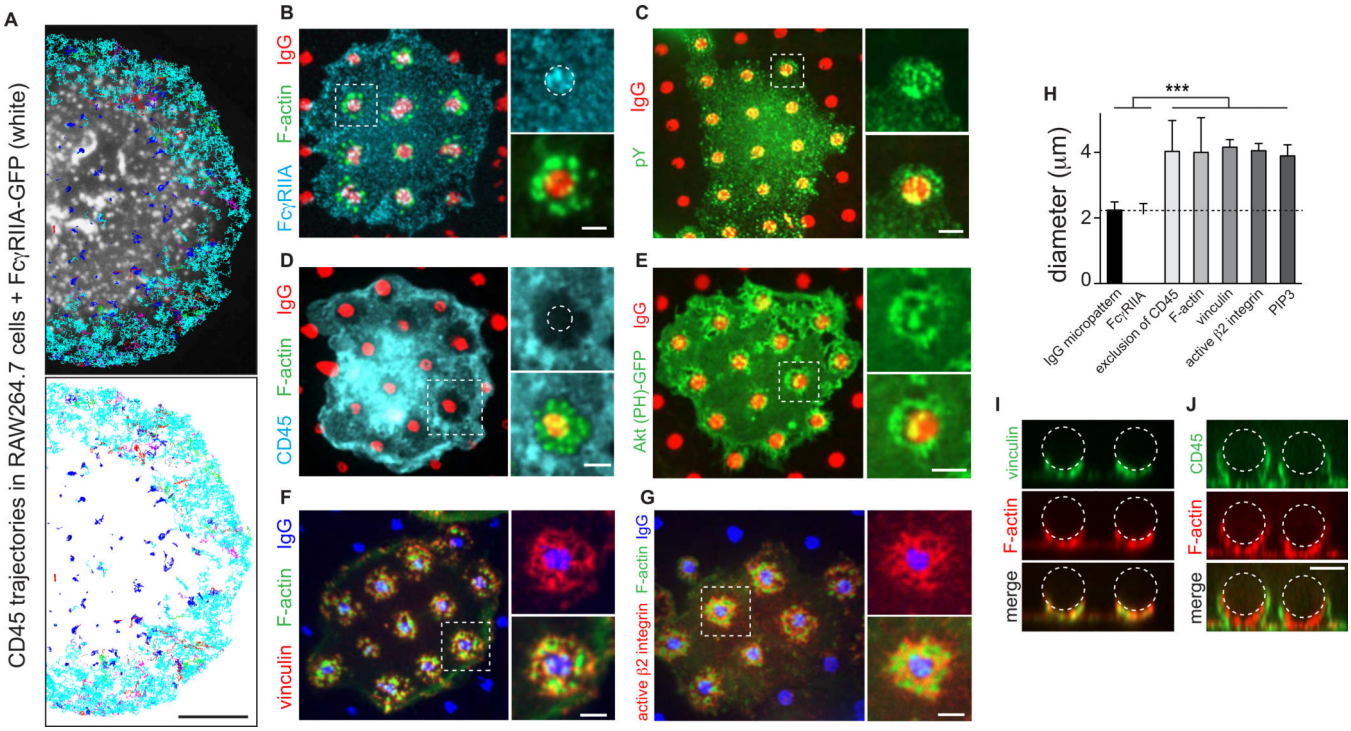

Fig. 3. CD45 depletion extends beyond regions of engaged Fcγ receptors and correlates with integrin adhesions

A) CD45 was labeled in RAW 264.7 cells expressing FcγRIIA-GFP using Qdots bound to anti-CD45 Fab fragments. CD45 trajectories from 20 s videos were classified as confined (blue), free (cyan), or linear (red) and overlaid on a single image of clustered FcγRIIA-GFP taken when SMT started. Scale bar =5 μm. **B–G)** Human macrophages seeded onto IgG (red in B–E; blue in F–G) micropatterned coverslips for 10 min. Cells were stained for F-actin (green in B,D,F,G), FcγRIIA or CD45 (cyan in B,D), pY (green in C), vinculin (red in F) or active β2 integrin (red in G). **E**) Cells transfected with Akt (PH)-GFP (green). Scale bars =2 μm. **H)** Maximum diameter of all signals from B–G determined for 3–5 micropatterned regions of IgG per cell for >30 cells from 3 independent experiments. Bars are mean ± SEM. **I–J)** *xz* sections of human macrophages incubated with IgG-opsonized beads. Cells were fixed after 45 s and stained for vinculin or CD45 (green) and F-actin (red). Beads indicated by dotted lines. Scale bar =5 μm.

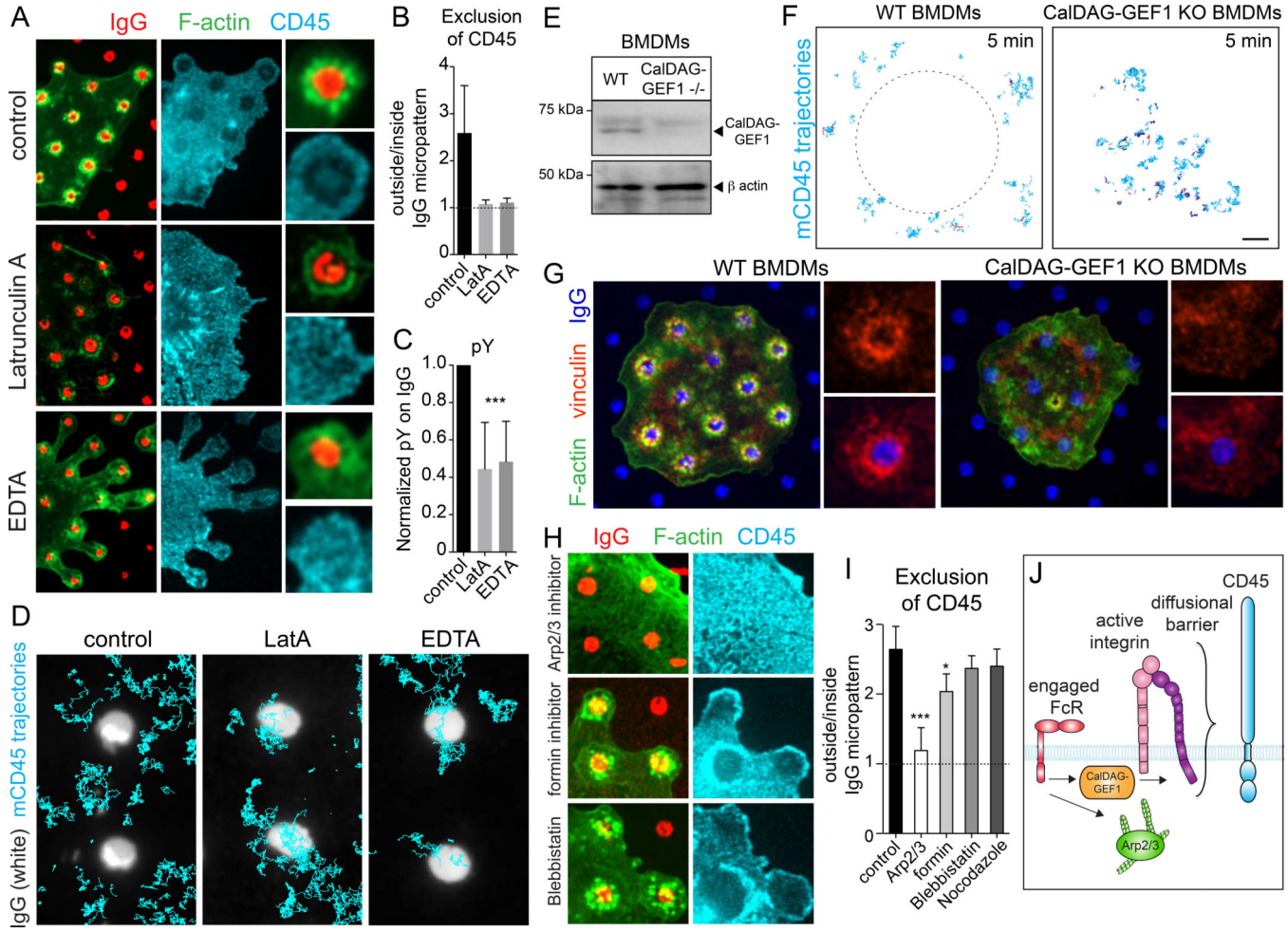

Fig. 4. Integrin activation and linkage to F-actin, mediated by CalDAG-GEF1 signaling, are required for CD45 exclusion

A–C) Human macrophages seeded onto micropatterned IgG (red) for 10 min before adding vehicle (top), 1 μM latrunculin A (middle), or 1.5 mM EDTA (bottom) for 3 min. Cells were fixed and stained for CD45 (cyan) and F-actin (green). In B, depletion was determined as a ratio of average CD45 signal intensity outside/inside micropatterned IgG regions. In C the pY signal was measured and normalized. B and C, means ± SEM of >30 cells from 3 independent experiments, each measuring 3–5 micropatterned IgG regions. **D)** Single CD45 molecules were labeled in macrophages using Fab fragments and Qdots. Cells were laid onto micropatterned IgG coverslips for 5 min before recording for 10 s at 33 Hz. Trajectories (cyan) are overlaid on a single image of the micropattern. **E)** BMDMs from wildtype (WT) or CalDAG-GEF1$^{-/-}$ mice were lysed and probed with indicated antibodies. **F)** Single CD45 molecules were labeled in WT or CalDAG-GEF1$^{-/-}$ BMDMs using Fab fragments and Qdots. Cells were laid onto IgG coverslips 5 min before recording for 10 s at 33 Hz. **G)** BMDMs were laid onto micropatterned IgG (blue) coverslips 5 min before staining for F-actin (green) and vinculin (red). **H–I)** Cells were incubated with vehicle, 10 μM Arp2/3 inhibitor (CK-666), 10 μM formin inhibitor (SMIFH2), 10 μM blebbistatin, or 1 μM nocodazole in suspension at 37°C in HBSS. Cells were then seeded onto coverslips,

stained and quantified as in A–B. **J)** Model for an integrin-dependent diffusional barrier initiated by FcγR engagement in macrophages. Scale bars =2 μm.

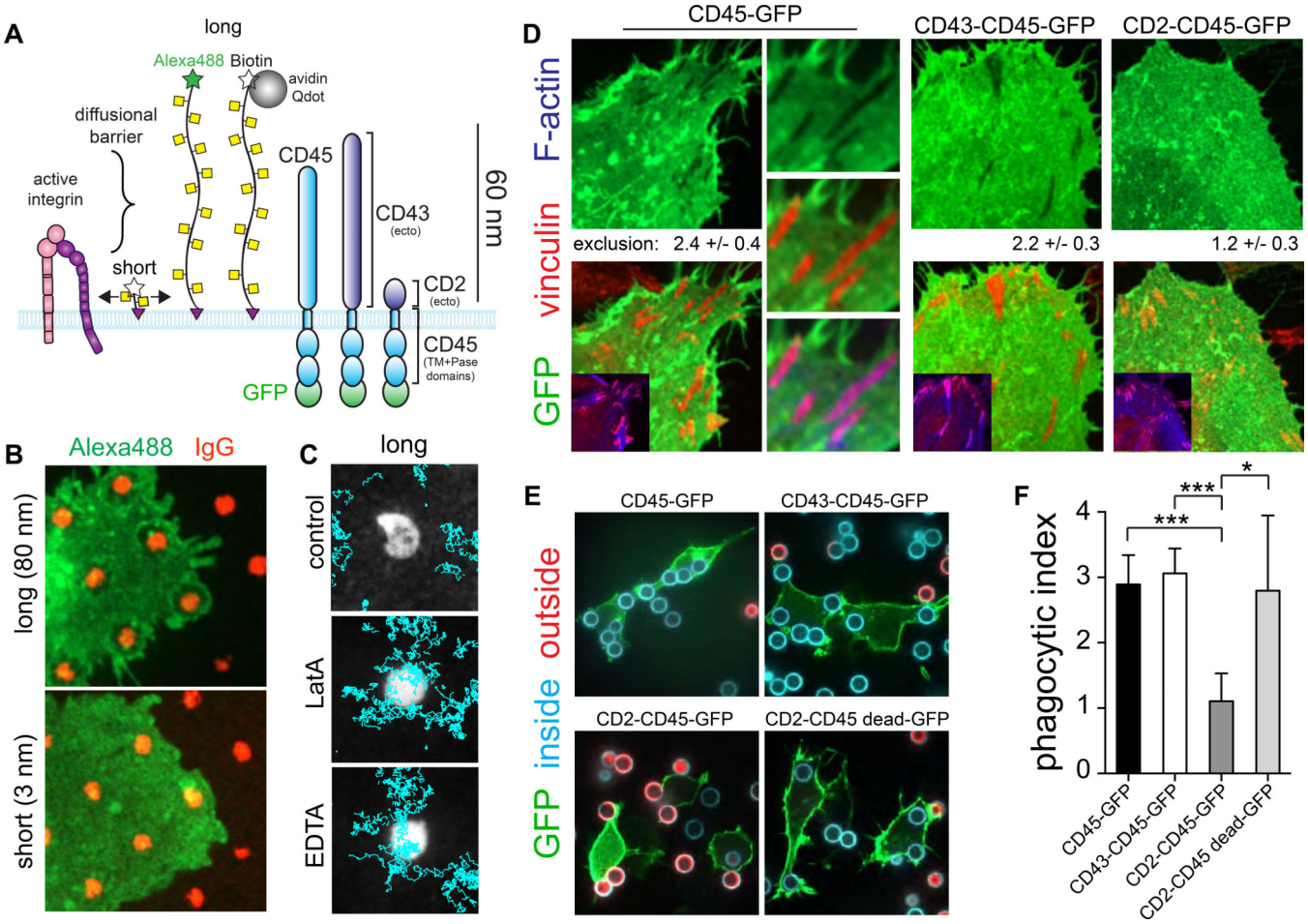

Fig. 5. Integrins exclude CD45 via an ectodomain size-based process required for phagocytosis

A) Comparison of the size of the ectodomain of an integrin heterodimer, short (3 nm) and long (80 nm) glycomimetic polymers, and CD43 and CD2 chimeric constructs used. **B)** Human macrophages incubated with 500 nM of either short or long Alexa488-conjugated glycomimetics for 20 min at 25°C before seeding onto micropatterned IgG (red) coverslips. Cells were imaged after 10 min. Scale bar =5 μm. **C)** Human macrophages were incubated with 10 nM of long biotinylated glycomimetic polymer for 20 min at 25°C then labeled with Qdots at 4°C. Cells were warmed to 37°C and seeded onto micropatterned IgG (white) and CD45 trajectories (cyan) recorded for 10 s at 33 Hz. Scale bar=2 μm. **D)** HeLa cells expressing the indicated GFP-tagged CD45 chimeric construct (green) fixed and stained for vinculin (red) and F-actin (blue). Mean ± SEM of exclusion determined as GFP signal intensity outside/inside 3–5 adhesions for >30 cells from 2 experiments. Scale bar =3 μm. **E)** RAW 264.7 cells expressing indicated fusion proteins, incubated with IgG-opsonized beads. Cells were first stained for accessible IgG (external beads, red), then permeabilized and stained for total IgG to determine internalized beads (cyan). Scale bar =10 μm. **F)** Phagocytic index determined as the mean number of internalized particles per cell for >100 cells from 3 independent experiments. Means ± SEM.

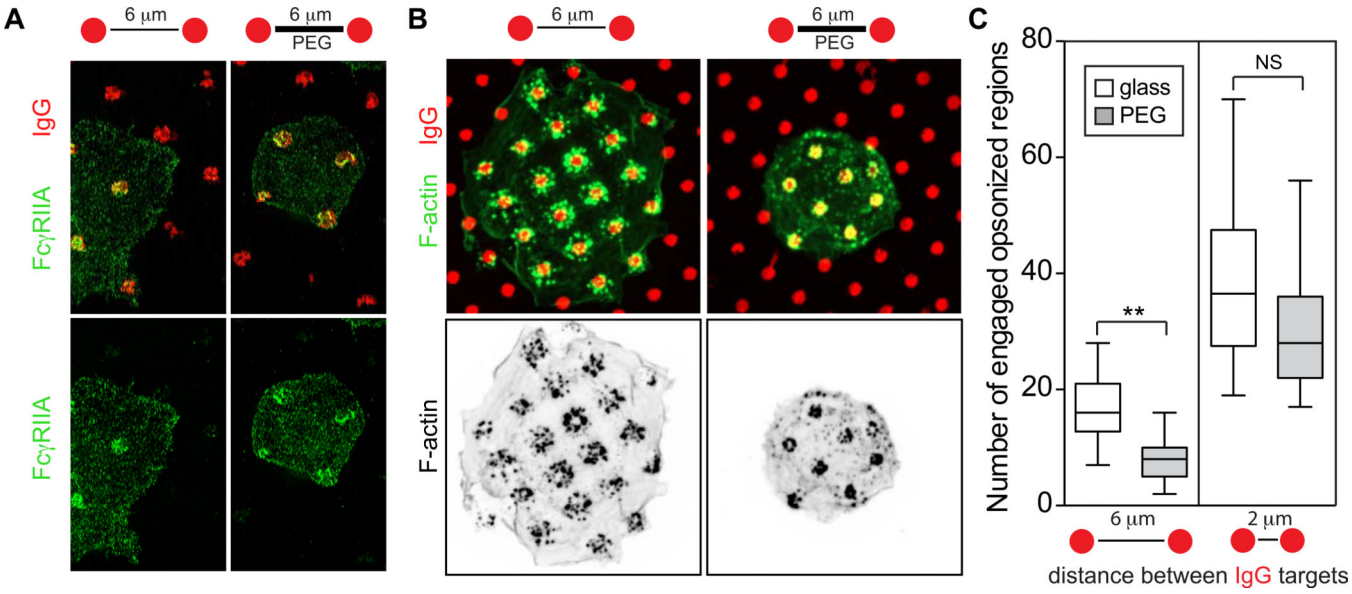

Fig. 6. Integrins facilitate engagement of distant points of opsonization

A) Human macrophages seeded onto micropatterned IgG spots (2 μm diameter) separated by 6 μm. The area of glass not covered by IgG was either left uncoated or was blocked with PEG. Cells were fixed after 2 min, stained for FcγRIIA and imaged by SIM. **B–C)** Cells were seeded as in A for 10 min on coverslips micropatterned with IgG spots separated by 2 or 6 μm before fixing and staining for F-actin. Representative experiment with 6 μm spacing is shown in B, with inverse coloring of the F-actin channel in black and white at bottom. C) Number of engaged opsonized spots. Means ± SD for >50 cells from 3 experiments. Scale bars =10 μm.

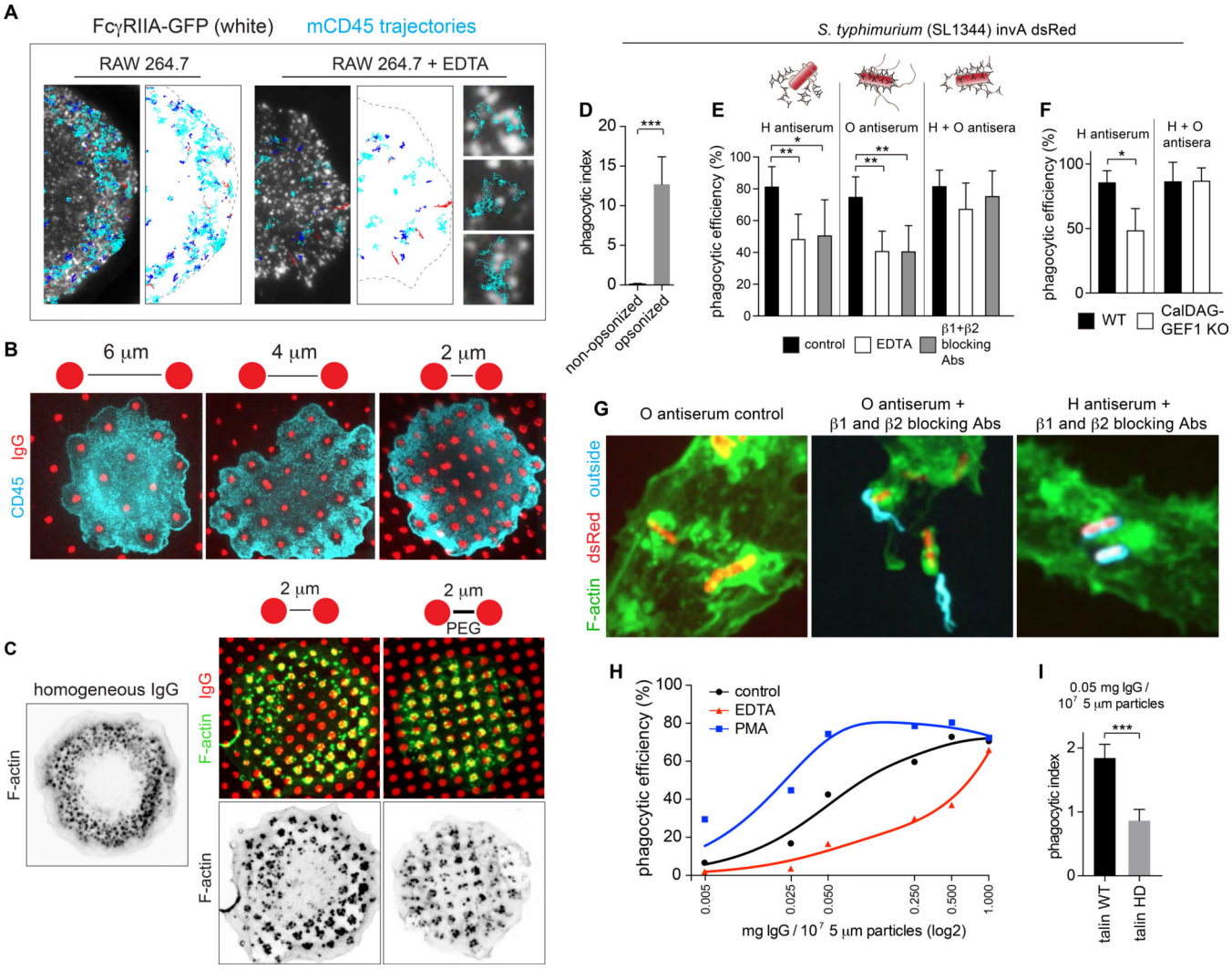

Fig. 7. Integrins coordinate points of opsonization for a uniform phagocytic response

A) CD45 was labeled for SMT in RAW 264.7 cells expressing Fcγ IIA-GFP. Cells were laid over IgG-coated coverslips for 5 min before treating with 1.5 mM EDTA (right). CD45 trajectories from 20 s videos were classified as confined (blue), free (cyan), or linear (red) and overlaid on a single image of clustered FcγRIIA-GFP. Scale bar =5 μm. **B)** Human macrophages were seeded onto IgG micropatterns separated by 6, 4, or 2 μm and after 10 min, fixed and stained for CD45 (cyan). Scale bar =10 μm. **C)** F-actin distribution on homogenously coated IgG (left) or on micropatterns separated by 2 μm of uncoated glass (middle) or PEG-treated glass (right). Scale bar =10 μm. **D)** Human macrophages were incubated with a non-invasive strain of *Salmonella* that was unopsonized or opsonized with O antiserum. Bars represent mean phagocytic index or number of internalized bacteria per cell ± SEM for >50 cells from 3 independent experiments. **E)** Human macrophages pretreated with EDTA for 2 min or integrin blocking antibodies for 10 min were incubated with bacteria opsonized with H, O, or H + O antisera. Non-internalized regions of bacteria were stained with H + O antisera and secondary antibodies before cells were permeabilized and stained for F-actin. Bacteria were detected by expression of dsRed. The number of

completely engulfed bacteria, expressed as a percentage of the total bound, was then determined. Bars are means ± SEM of data from >100 cells from 3 independent experiments. **F)** BMDMs from WT or CalDAG-GEF1$^{-/-}$ mice were incubated with bacteria opsonized with H or H + O antisera. **G)** Representative images from (E). Scale bar =5 μm. **H)** Human macrophages incubated with beads opsonized with the indicated concentrations of IgG in the presence of either vehicle, PMA or EDTA for 10 min. Data represent mean phagocytic efficiency (beads internalized/beads bound) from 30 cells. **I)** RAW 264.7 cells expressing full-length talin-GFP or talin head domain-GFP were incubated with opsonized microspheres for 10 min and the phagocytic index determined. Bars are means ± SEM of data from >50 cells from 3 independent experiments.